

## Transverse densities and parton distributions in the nucleon's chiral periphery

---

**Carlos Granados\***

*Uppsala Universitet, Uppsala, Sweden*

*E-mail: Carlos.Granados@physics.uu.se*

For hadrons, transverse densities are realized as proper densities when their structure is studied within the light front formulation of their internal dynamics. We calculate transverse densities from form factors decomposing the electromagnetic current and energy momentum tensor of the nucleon as projections of local products of light cone wave functions (LCWFs) of pion-nucleon systems. In our results, from a partonic interpretation, a mechanical picture of the nucleon emerges at its periphery in which the structure and dynamics are dictated by  $\chi$ EFT. The local products of LCWFs are generalized parton distributions (GPDs), and as such we further utilized them in characterizing and quantifying the dynamics of peripheral partons and its contribution to the nucleon's intrinsic properties, e.g., to its spin via orbital angular momentum. For transverse densities, this relation emphasizes their universality which makes them a natural subject to be studied in high and low energy experiments which are sensitive to the nucleon's chiral periphery.

*XXII. International Workshop on Deep-Inelastic Scattering and Related Subjects,  
28 April - 2 May 2014  
Warsaw, Poland*

---

\*Speaker.

## 1. Definition

Transverse densities are computed from two-dimensional Fourier integrals of form factors [1],

$$\rho(b) \equiv \int \frac{d^2\Delta_\perp}{2\pi} e^{i(b_\perp \cdot \Delta_\perp)} F(\Delta^2 = -\Delta_\perp^2). \quad (1.1)$$

They describe distributions projected on the nucleon's transverse plane. While three-dimensional Fourier integrals of form factors are approximated in very restrictive kinematics (static target) to three-dimensional densities, transverse densities as defined in Eq.(1.1) are boost invariant and quantify accordingly charge and current distributions within the nucleon in impact parameter space. They decompose the electromagnetic current density matrix in spin-independent ( $\rho_1$ ) and spin dependent ( $\tilde{\rho}_2 \equiv \frac{1}{2M_N} \frac{\partial \rho_2}{\partial b}$ ) terms, with the former being the transverse density associated to Dirac's form factor, and the latter computed from the transverse density of Pauli's form factor. It can be stated that this decomposition permits a mechanical interpretation of the nucleon as a classical pion-nucleon system, but one in which the pion is relativistic. One arrives to this result after calculating  $\rho_1$  and  $\tilde{\rho}_2$  using either an axial-vector or pseudo-scalar pion-nucleon couplings and noting that for both choices one finds that  $\rho_1 < \tilde{\rho}_2$ . We present both approaches below and also emphasize the extent of their numerical agreement and comment on the origin of their discrepancy. We also extend this methodology into calculating transverse densities associated to the form factors of the energy momentum tensor from which we define a transverse density of orbital angular momentum and compute it in the chiral region.

## 2. Spectral functions and parametric regions from $\chi$ EFT

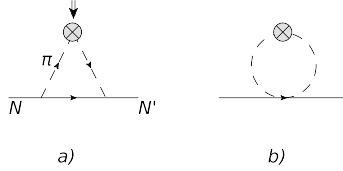


**Figure 1:** Leading chiral contributions to the isovector nucleon form factor. a) Diagram with intermediate nucleon (baryon). b) Contact term diagram.

The dynamics in the nucleonic periphery is governed by chiral effective field theory  $\chi$ EFT in which pions ( $\pi$ ), and nucleons ( $\psi$ ) constitute the fundamental degrees of freedom. Starting from a general  $\chi$ EFT Lagrangian (see e.g., [2], and keeping the leading terms in powers of the pion field, one works with the interaction Lagrangian,

$$\mathcal{L}_{\pi\mathcal{N}} = -\frac{g_A}{F_\pi} \bar{\psi} \gamma^\mu \gamma_5 \tau^a \psi \partial_\mu \pi^a - \frac{1}{4F_\pi^2} \bar{\psi} \gamma^\mu \tau^a \psi \varepsilon^{abc} \pi_b \partial_\mu \pi^c \quad (2.1)$$

which provides axial-vector and contact term interactions in the pionic contribution to the nucleon's electromagnetic current. The leading diagrams are shown in Fig.(2). Diagram a) can be decomposed into a propagating term and a contact term which combined with diagram b) results in a total contact term contribution proportional to  $1 - g_A$ . This contribution is absent for the Pauli

form factor hence it also does not contribute to  $\rho_2$ , while it amounts to less than 10% of the total contribution to  $\rho_1$ . Through the dispersion integral,

$$\rho(b) = \int_{4M_\pi^2}^{\infty} \frac{dt}{2\pi} K_0(\sqrt{tb}) \frac{\text{Im}F(t+i0)}{\pi}, \quad (2.2)$$

transverse densities are calculated using the imaginary part of the form factors which are obtained by using Cutkosky rules on the two pion cut of the diagrams in Fig.2 [3][4]. The modified Bessel functions  $K_0(\sqrt{tb})$  in Eq.(2.2) behave asymptotically as  $\frac{e^{-2\sqrt{tb}}}{\sqrt{tb}}$ , effectively parameterizing in  $b$  different kinematic regions of the nucleons large distance structure.

Through  $b$ , transverse densities filter out the dynamics associated with high momentum modes ( $\sqrt{t} > \frac{1}{b}$ ) which combined with the analytic structure of the form factors within the particle exchange picture permits one to identify the above mentioned parametric regions. For the particular case of the two pion exchange contribution to the isovector form factors, one can identify a molecular region at  $b \sim O(M_N^2/M_\pi^3)$  [4], dominated by a subthreshold singularity ( $t_{sub} = 4M_\pi^2 - M_N^4/M_N^2$ ); an endpoint singularity in the pion nucleon scattering amplitude which shows up in the analytic structure of the form factor and limits the convergence of kinematic series near threshold [2].

Another parametric region is identified at  $b \sim O(1/M_\pi)$  (chiral region). Momentum modes with  $t - 4M_\pi^2 \sim O(M_\pi^2)$  contribute the most to the transverse densities in this region. In a partonic picture of the nucleon, this region will be populated by pions with characteristic momenta of order  $M_\pi$ . A heavy baryon expansion was developed for this region for both form factors which allowed approximating the corresponding transverse densities to analytic expansions in  $(M_\pi/M_N)$  and that resulted in good agreement with the densities computed through numerical integration. When compared with each other, the leading components of each expansion, for  $\rho_1$  and  $\tilde{\rho}_2$ , are at a ratio  $1:(O(M_\pi/M_N))$  respectively. This ratio will be connected through the light cone formulation addressed in the following section to a mechanical picture of a pion-nucleon system with total quantum numbers corresponding to a nucleon.

Lastly, it should be noted that from phenomenological studies the two pion contribution to the nucleon's isovector form factor quantified using  $\chi EFT$  as described above becomes only dominant in the region  $b > 2fm$ [3]. For smaller distances, the isovector form factor is mostly contributed by heavier non-chiral exchange mechanisms that fall rapidly in the chiral region.

### 3. Light cone wave functions and $\pi$ -parton distributions

To leading order in pion fields, most of the contribution of the pion current comes from the propagating part of the diagram in Fig.(2a). This propagating part is the only contribution if one starts the derivation with a  $\pi N$  pseudo scalar coupling, and is also the only term in a light cone time-ordered decomposition that can be cast in terms of an overlap of wave-functions of a  $\pi N$  system. Other terms vanish in the  $\Delta^+ = 0$  reference frame.

While the light cone electromagnetic current and the electromagnetic form factors of the nucleon are given as overlap of LCWFs in relative transverse momentum  $k_\perp$ , the corresponding transverse densities can be written as y-integrals of local products of LCWFs in transverse position [1][8].

$$\rho_1(b) = \int \frac{dy}{2\pi} \left[ \frac{1}{(1-y)^2} \left( \Psi_N^\dagger(y, \vec{b}') \Psi_N(y, \vec{b}') \right)_{\lambda=\lambda'=+} + (1-g_A)\delta(y)C.T. \right]$$

$$\tilde{\rho}_2(b) = 2 \int \frac{dy}{2\pi} \frac{1}{(1-y)^2} \left( \Psi_N^\dagger(y, \vec{b}') \Psi_N(y, \vec{b}') \right)_{\lambda=-\lambda'=-}, \quad (3.1)$$

in which  $b' = b/(1-y)$ ,  $y$  is the light cone momentum fraction of  $\pi N$  system carried by the pion and  $\lambda$  and  $\lambda'$  are the total spin of the system and the spin of the nucleon(baryon) respectively.

The contact term (*C.T.*) in Eq.(3.1) appears if one uses a pion-nucleon interaction with axial coupling, which is the case when this is derived from a chiral symmetric Lagrangian such as Eq.(2.1). This term is interpreted as non-partonic contributions to the nucleon current, and thus lives in the  $y \rightarrow 0$  region of what will be defined below as chiral parton distributions. It has also been noted that the contact term masks contributions from heavier baryon components to the nucleon wave function, and that if all these components were taken into account, the delta function of such contact term will be replaced by a broader distribution [3] that can in turn be absorbed in the wave function terms of the above equation.

In the case of the pion current contribution to the electromagnetic iso-vector transverse densities, the LCWFs in the above equations are written for a pion-baryon system with the intrinsic quantum numbers of the nucleon. These wave functions are eigenstates of an interaction Hamiltonian with pseudo-scalar pion-nucleon coupling. To leading order, the transverse densities derived from these wave functions through Eq.(3.1) can be written in terms of the real scalar functions [5]  $\psi_{0(1)}(y, r_\perp) \sim K_{0(1)}(\tilde{M}(y)r_\perp)$ :

$$\begin{aligned} \rho_1(b) &= \int \frac{dy}{2\pi} \frac{1}{(1-y)^2} (\psi_0^2(y, b') + \psi_1^2(y, b')) \\ \tilde{\rho}_2(b) &= 2 \int \frac{dy}{2\pi} \frac{1}{(1-y)^2} \psi_0(y, b') \psi_1(y, b'). \end{aligned} \quad (3.2)$$

From Eq.(3.2), one can see that  $\rho_1 \geq \tilde{\rho}_2$  and that the light-cone current is positive definite. Furthermore, in the chiral parametric region, through a heavy baryon expansion, one can show that  $\frac{\tilde{\rho}_2}{\rho_1} \sim O(1)$  [5][4]. Classically, this ratio corresponds to the velocity of charge carriers in a continuous current flux. In a simple mechanical picture of a weakly interacting pion-nucleon system, the lowest allowed orbital angular momentum component that contributes to 1/2 as the total angular momentum is  $l=1$ , which for a relative distance that falls within the chiral region ( $\sim M_\pi^{-1}$ ) corresponds to a pion moving nearly at the speed of light relative to the center of mass of the pion nucleon system. Hence, its momentum is relativistic ( $\sim M_\pi$ ).

The connection to a mechanical model described above is thus implicit in the light-cone description of the pion-nucleon component of the nucleon Fock wave function expansion which gives the proper meaning to densities in the classical quantum mechanical sense as it is shown in Eqs.(3.1). Having identified pions in the nucleon's chiral region as quasi-free particles, is natural to recognize the integrands of Eqs.(3.1) as parton distributions of pions, e.g.,  $f_1^\pi$  and  $f_2^\pi$ ,

$$\begin{aligned} f_1^\pi(y) &= \frac{1}{2\pi} \frac{1}{(1-y)^2} \left( \Psi_N^\dagger(y, \vec{b}') \Psi_N(y, \vec{b}') \right)_{\lambda=\lambda'=+} + (1-g_A)\delta(y)C.T. \\ f_2^\pi(y) &= 2 \frac{1}{2\pi} \frac{1}{(1-y)^2} \left( \Psi_N^\dagger(y, \vec{b}') \Psi_N(y, \vec{b}') \right)_{\lambda=-\lambda'=-} \end{aligned} \quad (3.3)$$

which are therefore computed in the periphery in a model independent manner through leading diagrams in  $\chi PT^1$ . Results are plotted in Fig.(2).

<sup>1</sup>See e.g., Ref. [6] in which these distributions are computed from the operator definitions of GPDs.

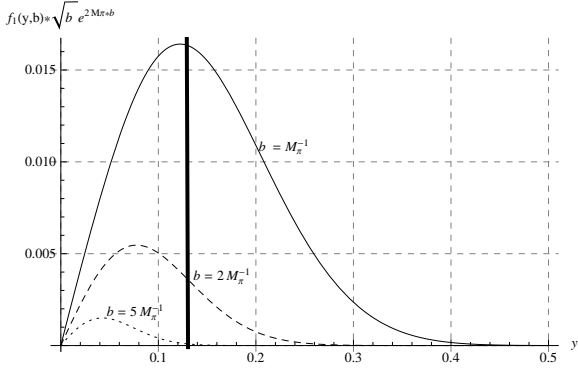


**Figure 2:** Distribution of parton-like pions in the chiral periphery of the nucleon. The bold vertical line indicates  $y = \frac{M_\pi}{M_N}$ , highlighting that this region is dominated by pions with  $y \sim O\left(\frac{M_\pi}{M_N}\right)$ . This trend shifts towards smaller values of  $y$  as the distribution is sample in larger  $b$  regions.

#### 4. EMT transverse densities and orbital angular momentum

One can further develop a quantifiable partonic description of the nucleon's structure at transverse distances of chiral order which can provide the parametric contribution from peripheral pions to the nucleon's intrinsic physical properties such as mass and spin. These properties are commonly related to the nucleon's compositeness or internal structure through the form factors that decompose covariantly the matrix elements of the energy momentum tensor and as it is the case for the electromagnetic form factors, they are functions of the square of the four-momentum difference between initial and final state,

$$\langle N' | \Theta^{\mu\nu} | N \rangle = \hat{u}(p') \left[ P^{(\mu} \gamma^{\nu)} A(\Delta^2) + \frac{P^{(\mu} \sigma^{\nu)\alpha} q_\alpha}{2M_N} B(\Delta^2) + \dots \right] u(p). \quad (4.1)$$

Of particular interest is the proton's spin which is given by form factors  $A$  and  $B$  through,

$$J_N = \frac{1}{2}(A(0) + B(0)), \quad (4.2)$$

From a proposed form factor associated with orbital angular momentum operator and that satisfies Eq.(4.2) [7], one can then find a transverse density of angular momentum in impact parameter space through transverse densities associated with form factors  $A$  and  $B$  [8].

$$\rho_J(b) = \frac{1}{3} \left[ (\rho_A(b) + \rho_B(b)) - b \frac{\partial}{\partial b} (\rho_A(b) + \rho_B(b)) \right] \quad (4.3)$$

Thus providing an additional tool in phenomenological studies for exploring the origin of the nucleon's spin.

Analogously to the case of transverse densities from electromagnetic form factors,  $\rho_A$  and  $\rho_B$  have been computed from the spectral functions or imaginary parts of form factors  $A$  and  $B$  through Eq.(2.2). These spectral functions in turn, are calculated using a  $\chi PT$  expansion of Eq.(4.1) [8]. To leading order in powers of the pion fields, only a diagram such as Fig.(2a) contributes while contact terms are absent from form factors  $A$  and  $B$ . Just as for the spectral functions of electromagnetic form factors, those for  $A$  and  $B$  possess a rich analytic structure which is also sampled or parameterized by the corresponding transverse densities within the same parametric regions discussed above. Thus, because the diagram studied from which both electromagnetic and energy momentum

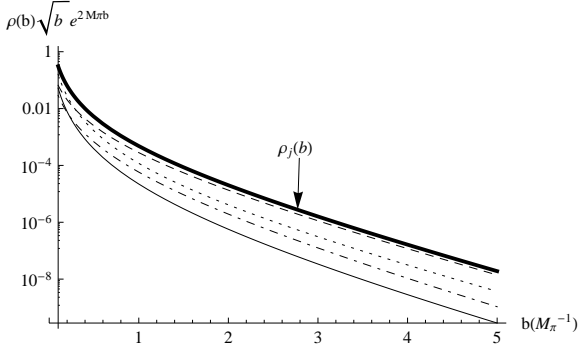


**Figure 3:** Scaled transverse densities from EMT form factors and of orbital angular momentum in the nucleon's chiral region. (Continuous)  $\rho_A$ , (dot-dashed)  $\rho_B$ , (dotted)  $-b \frac{\partial}{\partial b} \rho_A$ , (dashed)  $-b \frac{\partial}{\partial b} \rho_B$  and (bold)  $\rho_J$ .

tensor are computed factors in the same  $\pi N$  scattering amplitude, for  $A$  and  $B$  one finds a threshold singularity at the same position as for  $F_1$  and  $F_2$ . Again, just as the light-cone current is decomposed in spin independent  $\rho_1$  and spin-dependent  $\tilde{\rho}_2$  transverse densities, the  $++$  component of matrix elements of the energy momentum tensor are likewise decomposed in spin-independent  $\rho_A$  and spin-dependent  $\tilde{\rho}_B$  transverse densities that can also be written as local products of  $\pi N$  LCWFs,

$$\begin{aligned} \rho_A(b) &= \frac{3}{2} \int \frac{y}{(1-y)^2} \left( \Psi_N^\dagger(y, \vec{b}') \Psi_N(y, \vec{b}') \right)_{\lambda=\lambda'=++} \\ \tilde{\rho}_B(b) &= 3 \int \frac{dy}{2\pi} \frac{y}{(1-y)^2} \left( \Psi_N^\dagger(y, \vec{b}') \Psi_N(y, \vec{b}') \right)_{\lambda=-\lambda'=-}, \end{aligned} \quad (4.4)$$

which as expected are proportional to moments of the parton distributions associated with  $\rho_1$  and  $\tilde{\rho}_2$  (see Eq.(3.3)). The computed densities are plotted in Fig. (3) which shows clearly that  $\rho_J$  is dominated by  $-b \frac{\partial}{\partial b} \rho_B$  in the chiral region.

It is also worth pointing that there is no contact term contributions to  $\rho_A$  or  $\rho_B$  using either axial vector or pseudoscalar coupling, thus both choices result in the same transverse densities. This is clear if one just calculate the second moments in  $y$  of the parton distributions given in Eq.(3.3). Contact terms of order  $g_A$  may be present in other form factors decomposing EMT (columns in Eq.(4.1)). Understanding their origin and a physical interpretation in studies of the nucleons peripheral structure are under way and may shed light into effectively quantifying the composite nature of the nucleon.

## References

- [1] G. A. Miller, Ann. Rev. Nucl. Part. Sci. **60**, 1 (2010) [arXiv:1002.0355 [nucl-th]].
- [2] T. Becher and H. Leutwyler, Eur. Phys. J. C **9**, 643 (1999) [hep-ph/9901384].
- [3] M. Strikman and C. Weiss, Phys. Rev. C **82**, 042201 (2010) [arXiv:1004.3535 [hep-ph]].
- [4] C. Granados and C. Weiss, JHEP **1401**, 092 (2014) [arXiv:1308.1634 [hep-ph], arXiv:1308.1634].
- [5] C. Granados and C. Weiss, Int. J. Mod. Phys. Conf. Ser. **25**, 1460036 (2014) [arXiv:1310.0739 [hep-ph]].
- [6] M. Strikman and C. Weiss, Phys. Rev. D **69**, 054012 (2004) [hep-ph/0308191].
- [7] M. V. Polyakov, Phys. Lett. B **555**, 57 (2003) [hep-ph/0210165].
- [8] C. Granados and C. Weiss, in preparation.